NUMERICAL SIMULATIONS OF GASEOUS COMPOUND DISPERSION AROUND A CUBIC OBSTACLE UNDER DIFFERENT ATMOSPHERIC STABILITY CONDITIONS: USE OF k-ω SST TURBULENCE MODELLING

I.B. Costa[a], isbahia@hotmail.com
B. Furieri[b], furieribruno@gmail.com
[a]Universidade Federal do Espírito Santo, Av. F. Ferrari, 514, Goiabeiras, Vitória, 29075-910, Brazil
[b]Instituto Federal do Espírito Santo, Av. Vitória, 1729, Jucutuquara, Vitória, 29046-020, Brazil

N. C. Reis[a], neyval@gmail.com
J. M. Santos[a], jmerisantos@yahoo.com.br
H. Dourado[c], harerton@terra.com.br
[c]Faculdades Integradas de Aracruz, Rua Prof. Berilo Basílio dos Santos, Centro, Aracruz, 29194-910, Brazil

Abstract. *Wind flow and dispersion of gaseous emissions in the near wake of an isolated cubic building under stable, neutral and unstable atmosphere conditions were investigated using the k-ω SST turbulence modelling. Generally, RANS turbulence models overestimate the length of the recirculation zone downstream of a building. This is significantly affected by the turbulent kinetic energy production at the stagnation zone. In order to control this deficiency, the Production Limiter function (implemented in Ansys Fluent) was employed, with the purpose of restricting the turbulent kinetic energy production term. It allows a reduction in turbulence viscosity level and improves the prediction of separation zones. The numerical results were compared with wind tunnel experiments carried out by Yassin (2013). The Richardson bulk (Ri_B) and Reynolds numbers (Re_b) for each test case are: (i) stable: $Ri_B = 0.023$ and $Re_b = 5.1 \times 10^3$, (ii) neutral: $Ri_B = 0.0$ and $Re_b = 5.8 \times 10^3$, and (iii) unstable: $Ri_B = -0.016$ and $Re_b = 6.6 \times 10^3$. Source emission was located on the building roof. The results of the k-ω SST model showed good qualitative agreement, while some discrepancies from a quantitative point of view were observed with wind tunnel experimental results. However, the vertical profiles of mean longitudinal velocity presented high relative error close to the building. The compound dilution away from the building was also slightly overestimated. The calculated recirculation zone length is 1.93H.*

Keywords*: Pollutant dispersion, Atmospheric stability, CFD Models, isolated building, wake region, rooftop stack*

1. INTRODUCTION

The significant increase in air emissions from anthropogenic sources and the environmental impacts associated with the atmospheric dispersion of pollutants in urban areas has been the subject of extensive research in recent years (Henderson, 2013; Brusca et al., 2015; Bjorkegren et al., 2015). Air pollution is responsible for the changes of the physical, chemical or biological characteristics of the atmosphere, and the effects can range from damage to human health, animals, plants, or even affect the activities of the people and their welfare.

Contaminants in the atmosphere can be emitted in the form of particles or gases and the impact of air pollutants in the receptor result from the interaction of the source emission processes, dispersion and deposition. These processes are altered by the presence of obstacles that have particular characteristics which enhance dispersion.

Most studies on the mean flow and dispersion of pollutants in the vicinity of obstacles were held in neutral stability conditions (Hargreaves et al., 2007, Tominaga, 2015), and show that the main factors of the incident flow depend on the shape and orientation of the obstacle, the approaching flow characteristics and, as the diffusion process is affected, with the most important parameters to characterize the incident flow obstacle is the atmospheric stability (Santos, 2000). As results of Yassin (2013), the atmospheric stratification conditions can influence the dispersion, because it significantly changes the flow pattern around the buildings.

The prediction of flow and dispersion of pollutants around obstacles present major challenges for researchers, as experimental tests in the wind tunnel or field can be expensive, difficult to implement and of limited application. Mathematical modeling emerges as a procedure that has been studied to solve the problem of simulation of flow and dispersion based on the resolution of the governing equations of mass transport, momentum, energy and chemical species (Pope, 2000).

The flow around a building is typically turbulent, with enhanced mixing of fluid particles along the main flow direction due to random fluctuations in the three dimensional velocity fields.

The approaches used for different types of models that seek to represent the transport phenomena, mostly vary as to the complexity of the employed turbulence modeling, which is one of the biggest barriers to the most appropriate representations of reality by numerical models. More complex models, such as Large Eddy Simulation (LES) and Direct Numerical Simulation (DNS) may present better accuracy, but usually require intense computer power. Time

averaged equation models (or Reynolds averaged Navier-Stokes – RANS – models), such as k-Ɛ , k-ω and its variations (Jones and Launder, 1974; Menter, 1994), have been used to describe the turbulent flow and gas dispersion around obstacles, with satisfactory results (Xing et al., 2013; Rocha et al., 2014).

The present study investigates the dispersion of a pollutant emitted from the top of an obstacle under different atmospheric stability conditions using the behavior of the transport of ethylene gas composed around an obstacle in different conditions of atmospheric stability using the k-ω SST turbulence model developed by Menter (1994). The objectives are (i) to verify the length of the recirculation zone behind the building and (ii) to minimize the effects of overestimation of the turbulent kinetic energy production in the stagnant zones with use of production function limiter.

2. METHODOLOGY

2.1 Wind tunnel experiment

The wind tunnel experiments simulated in the present work were conducted at the Tokyo Polytechnic University, and are described in detail by Yassin (2013). Three different atmospheric stabilities were simulated: stable, neutral and unstable. The wind tunnel working section was 1.2 X 1.0 m and its length was 16.0 m. The wind tunnel consisted of a fan, temperature profile cart to measure vertical temperature, floor heating and cooling panels, and ambient air conditioner (Figure 1). Air temperature was controllable in the range 283.15 – 333.15 K. The experiments were conducted with an inlet wind velocity and air temperature of 1.3 m s^{-1} and 288.15 K.

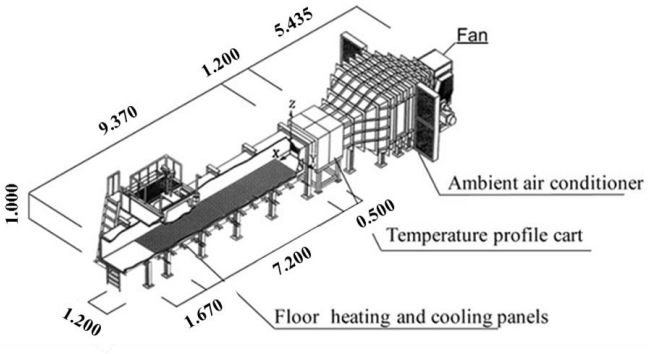

Figure 1. Wind tunnel representation thermally stratified. Yassin (2013).

The building model consisted of a cube with faces measuring 0.1 m. The stack was set at the center of the building roof, with a height of 0.007 m, and inner and outer diameters 0.004m and 0.006m, respectively. A split film was adopted for wind velocity measurement, and a 5-µm cold-wire thermometer was used for temperature measurement. Ethylene (C_2H_4) was used as tracer gas, released without buoyancy. A high-response hydrocarbon analyzer detector (Flame ionization detector, FID) was used to measure C_2H_4 concentration. Figure 2 shows vertical distributions of mean velocity, turbulence intensity and temperature in the simulated boundary layer for each thermal stability. x=0.0 is located at the downstream side of the obstacle. The profiles presented in Figure 2 are obtained in the input field at the coordinate x=-0.6m.

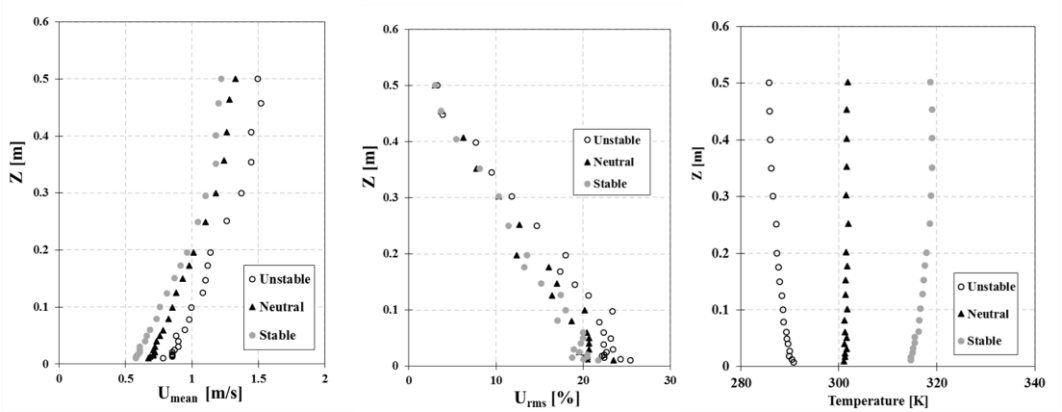

Figure 2. Vertical distributions of mean velocity, turbulence intensity and temperature in the simulated boundary layer under thermal stability.

2.2 Modelling tool

2.2.1 Computational tool

The Reynolds-Averaged equations for mass, momentum, energy and pollutant mass fraction were solved with ANSYS FLUENT 15.0, a CFD code which solves the transport equations numerically using the finite volume method for structured and non-structured meshes. Turbulence closure was obtained through the eddy viscosity concept. The simulations employed the k-ω SST model turbulence model. This model combine different elements of existing models and is considered superior to their RANS alternatives and leads to major improvements in the prediction of adverse pressure flows (Menter, 1994) Figure 3 shows a view of the central plan building (x- z) at y=0.0; also shown are the reference points where simulation results is compared to experimental data.

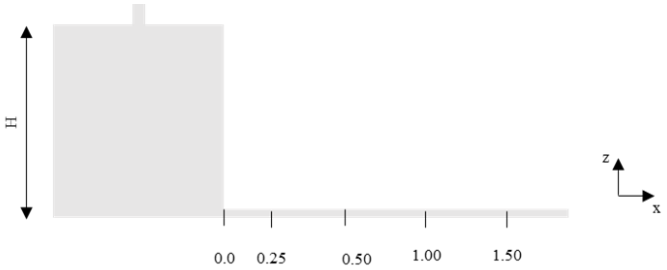

Figure 3. Building and stack models.

2.2.2 Grid and domain characteristics

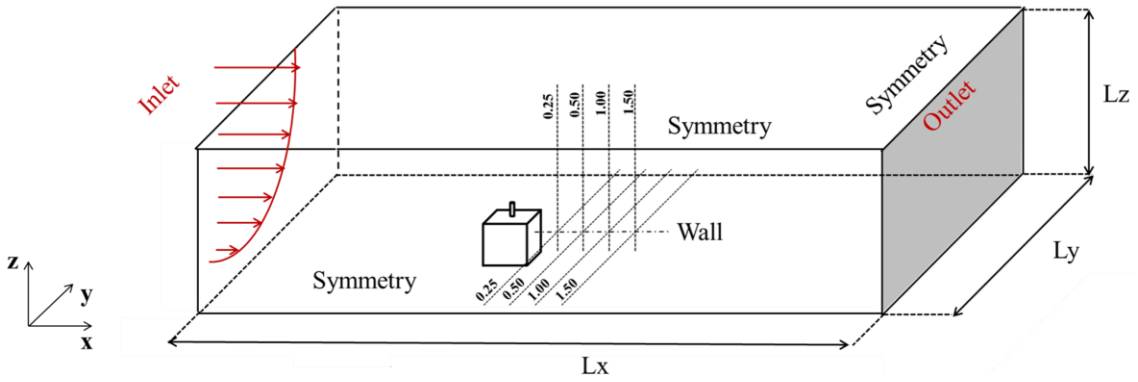

Figure 4. Representation of the computational domain.

The boundary conditions used in this study (Figure 4) are now described. Inlet: wind velocity, k and ω profiles; upper and side walls: symmetry; floor: no slip condition; outlet: Outflow condition. Table 1 shows Bulk Richardson number (RB) and Reynolds numbers (based on building and stack height, Reb & Res, respectively) for each atmospheric stability.

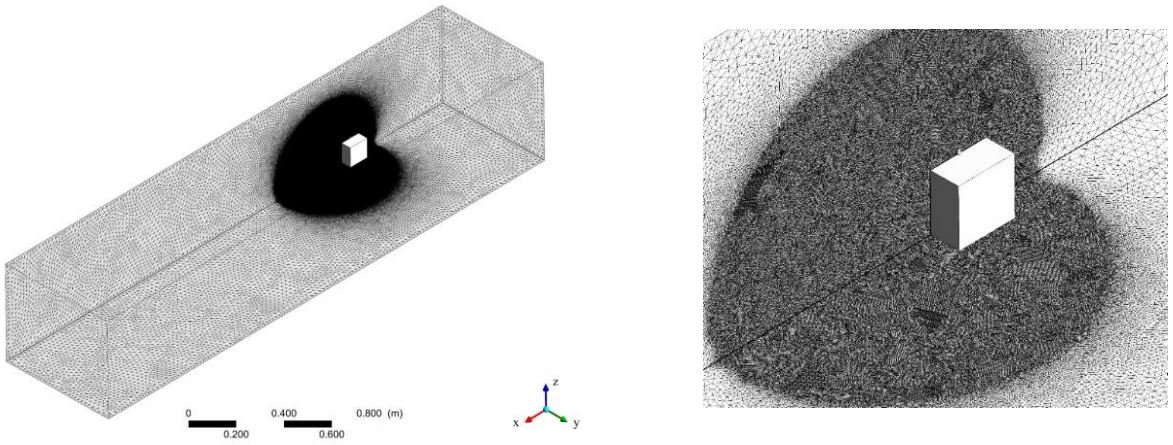

(a) (b)

Figure 5. Mesh employed in the numerical simulation. (a) Overview and (b) an enlarged view of the central plan, floor and building.

The unstructured mesh (Figure 5a) was generated using ANSYS MESHING 15.0 and consisted of 8 million tetrahedral elements. The mesh was refined near the obstacle (Figure 5b).

Table 1. Bulk Richardson number (R_B), building and stack Reynolds numbers (Re_b & Re_s) and flow/dispersion characteristics in stratified thermal stability.

Thermal stability	R_B	Re_b	Re_s
Stable	0.023	5.1×10^3	1.03×10^2
Neutral	0.000	5.8×10^3	1.20×10^2
Unstable	-0.016	6.6×10^3	1.30×10^2

3. RESULTS AND DISCUSSION

3.1 Flow field

3.1.1 Neutral condition

Figure 6 shows the longitudinal velocity field near the obstacle. A recirculation zone is evident downstream of the obstacle, characterized by negative along-flow velocities which increase dilution of the tracer gas. The reattachment point was located at 1.93H downwind the obstacle (Figure 7). Results show that the turbulence model was able to predict the major regions that occur in flow around a building.

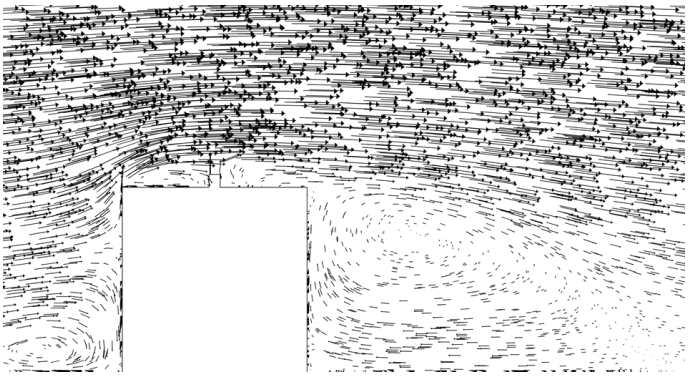

Figure 6. Representation of the velocity vectors in the central plane.

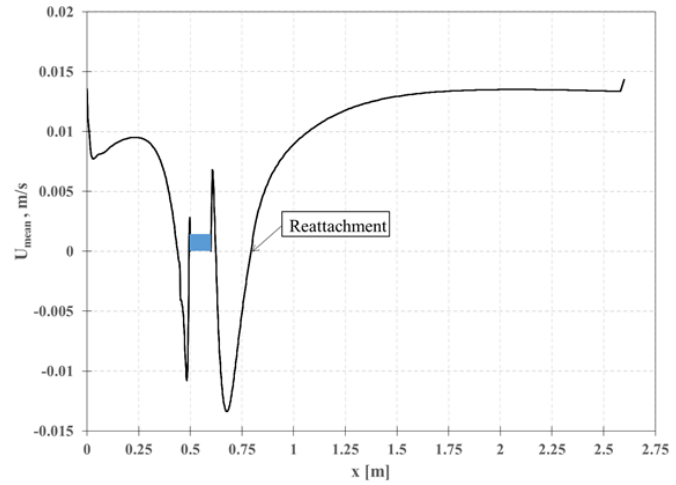

Figure 7. Profile of mean velocity in the main flow direction near the ground.

The k-ω SST model used in the present work employs mixing functions from the standard k-ω model close to the obstacle and from the standard k-ε model for the rest of the simulation domain. In addition, the use of the Production Limiter function included in ANSYS FLUENT, which restrain Turbulent kinetic energy (TKE) production in stagnation zones such as the obstacle windward wall, enhancing the prediction of the velocity field and hence, the separations zones of the flow around the obstacle. Following Valger et al. (2015) the TKE production due to shear stresses to specific dissipation rate ratio was set at 10 in the Production Limiter function. TKE levels in the symmetry plane (y/H = 0.0) are shown in Figure 8. There is a peak in TKE level in the upper edge of the windward building face. Correct prediction of TKE production influences the predicted anisotropy of the flow and, consequently, the length of the recirculation zone downwind the obstacle.

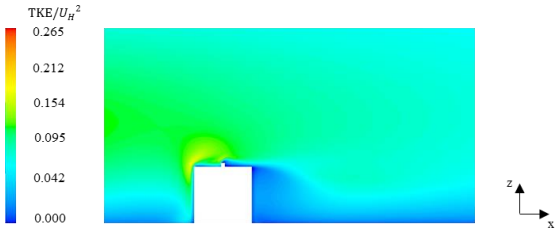

Figure 8. Vertical contour of Turbulent Kinetic Energy (TKE) non-dimensional with TKE at the height of the building.

Vertical profiles of the mean longitudinal velocity component are shown in Figure 9, comparing experimental and numerical simulation results at four different points downwind the obstacle. Simulation results present the same general trends as the experimental results. Close to the obstacle (x/H=0.25), the relative error was 0.271 while at the x/H=1.25, the relative error was 0.203. The better agreement of the results obtained at greater distances may be due to the lower anisotropy of the flow predicted by the model. The relative errors are acceptable when compared with a study by Tominaga (2015), which investigated the flow around isolated obstacles with different roof slopes in neutral atmospheric condition using the k-ω SST model, with results showing relative errors of 0.300 downstream of the block.

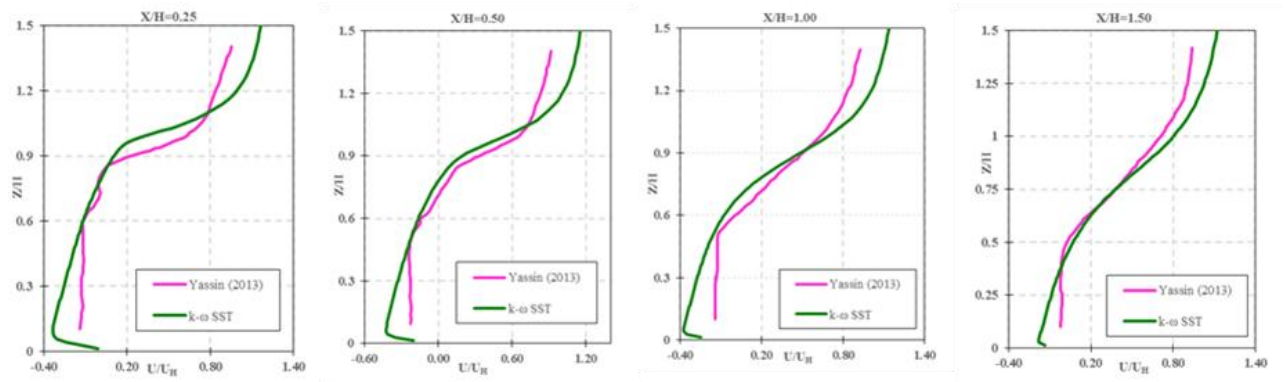

Figure 9. Vertical profiles of mean velocity component in the longitudinal direction at: x/H=0.25; x/H=0.50; x/H=1.00; x/H=1.50.

3.1.2 Comparison between neutral, unstable and stable conditions

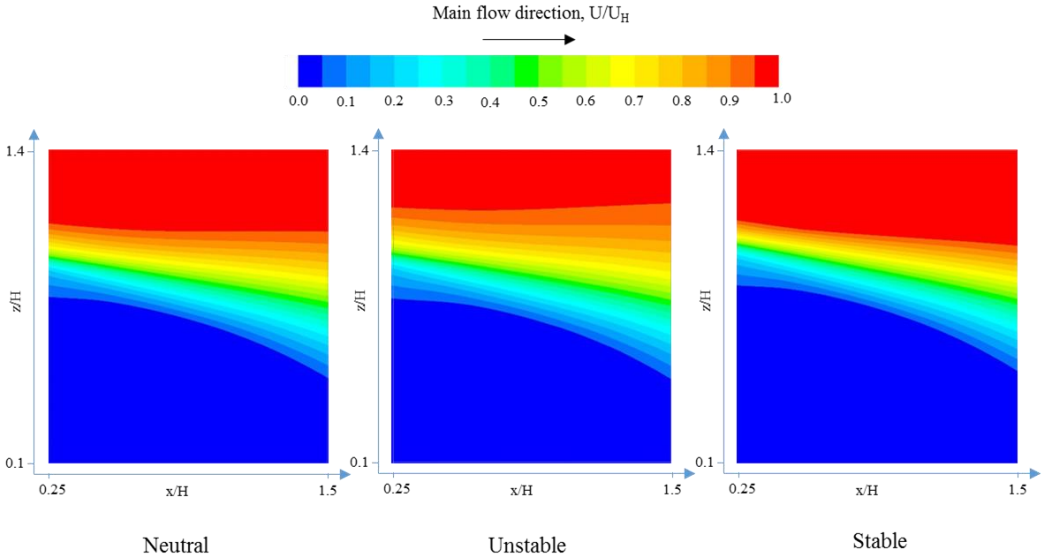

Figure 10. Contour of longitudinal velocity view of the central plane of the building, k- ω SST model.

Contours of longitudinal velocity near the turbulent wake for the different simulated atmospheric conditions are shown in Figure 10. Results of the numerical simulation are consistent when compared to the experimental results. Results for the stable condition shows less flow separation when compared to the neutral condition. The results are consistent with experimental and simulation results from previous studies which employed different turbulence models (Yassin, 2013; Mavroidis, 1999; Mavroidis, 2012; Cezana, 2007). Comparison of the mean wind velocity profiles at x/H = 0.25, x/H = 0.5, x/H = 1.00 and x/H = 1.50 is presented in Figure 11 showed little variation between each simulated atmospheric stability condition, possibly due to the small difference in stability between each simulated atmospheric condition, as shown in Table 1.

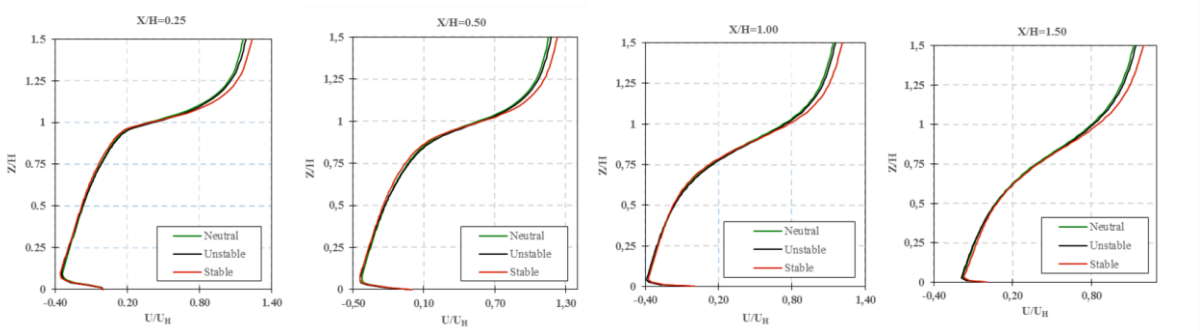

Figure 11. Vertical profiles of mean velocity component in the longitudinal direction for different conditions at: x/H=0.25; x/H=0.50; x/H=1.00; x/H=1.50.

3.2 Dispersion field

3.2.1 Neutral condition

Non-dimensional concentration results are calculated according to Equation (1):

$$K = \frac{C}{C_0} \tag{1}$$

Where C is the Ethylene mole fraction and C_0 is the Ethylene reference concentration, given by Equation (2):

$$C_0 = \frac{Q}{U_H H^2} \tag{2}$$

Where Q is Source volume flow rate and U_H is the Free stream velocity at building height H.

In RANS strategy governing equations are solved on ensemble average and turbulence is modelled using a term called turbulent viscosity. Simplification implies greater difficulty in representing the different wavelengths of turbulent flow which may not perfectly agree with experimental data. When comparing the model results used in this study to the experimental data it is possible to notice some differences. Figure 12 shows vertical mean concentration profiles. It can be stated that the highest concentrations level occurs at the same vertical position for both experimental and simulated results, however, results for the numerical simulation show greater dilution at x/H > 0.50. This effect is due to the fact that the large-scale transient fluctuations caused by vortex shedding the behind the obstacle cannot be reproduced by the steady-state RANS model.

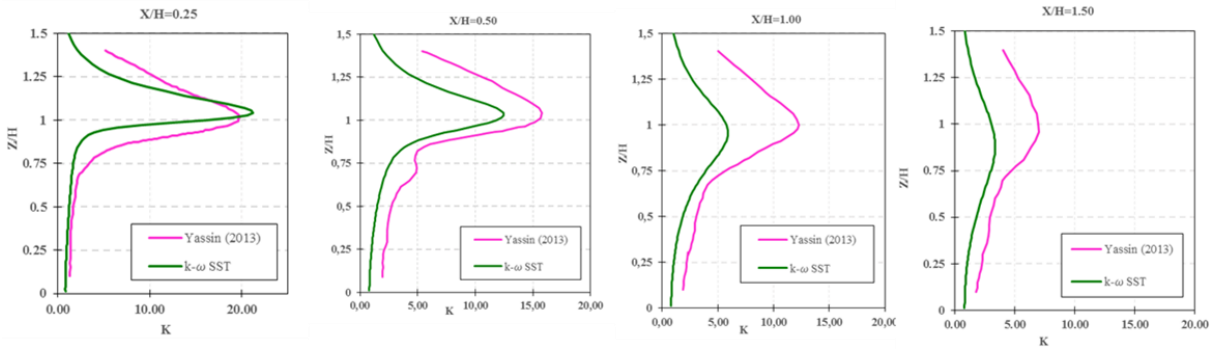

Figure 12. Vertical profiles of non-dimensional concentration, K, at: x/H=0.25; x/H=0.50; x/H=1.00; x/H=1.50.

3.2.2 Comparison between neutral, unstable and stable conditions

Figure 13 shows vertical profiles of mean concentration at different points of near wake for all simulated atmospheric conditions. It can be noted that the lowest concentrations were observed for the unstable condition, while the highest values were observed in the stable condition. This is a consequence of the higher turbulence levels of the unstable condition which enhance dilution of the tracer gas. For each stability condition, the highest concentration value was observed at the same vertical position.

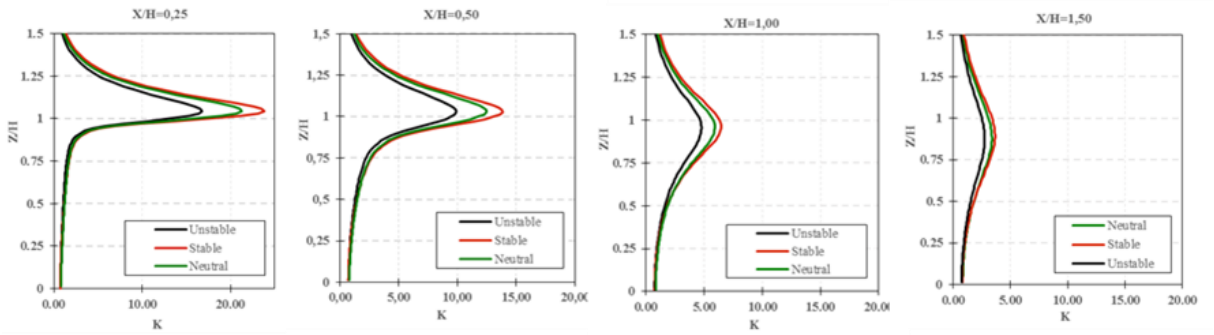

Figure 13. Vertical profiles of non-dimensional concentration, K, for different conditions at: x/H=0.25; x/H=0.50; x/H=1.00; x/H=1.50.

4. SUMMARY AND CONCLUSIONS

The present work investigated the flow and dispersion around an isolated cubic obstacle with different atmospheric conditions – stable, neutral, and unstable – through numerical simulations using the RANS based k-ω SST turbulence model. Results were compared to experimental wind tunnel data. The following aspects were revealed:

- Generally, the k-ω SST results agreed well with experimental data for the velocity and concentration; the prediction accuracy for those variables behind the building is poor, although compatible with previous studies. This effect is basically due to the fact that the large-scale transient fluctuations caused by vortex shedding behind the obstacle cannot be reproduced by the steady-RANS.
- The “production limiter” function provided the reduction of the TKE production in the stagnation zone and thus improving the results.

- Although the small variations between each atmospheric stability condition simulated had little influence in the mean flow velocities, concentration results reflected the different turbulence levels expected in each atmospheric condition. The results showed good agreement of the qualitative point of view, although the quantitative comparison presents some discrepancies probably because of the limitations of the RANS approach in the representation of turbulence.

5. ACKNOWLEDGEMENTS

The authors thank to FAPES, CAPES, and CNPQ for the financial support.

6. REFERENCES

Brusca, S.; Famoso, F.; Lanzafameb, R.; Garrano, A.M.C.; Monforte, P., 2015. "Experimental analysis of a plume dispersion around obstacles". ATI 2015 – 70th Conference of Engineering Association, No. 82, pp. 695-701.

Bjorkegren, A.B.; Grimmond, C.S.B.; Kotthaus, S.; Malamud, B.D., 2015. "CO_2 emission estimation in the urban environment: Measurement of the CO2 storage term". Atmospheric environment, No. 122, pp. 775-790.

Cezana, F. C., 2007. Simulação numérica da dispersão de poluentes ao redor de um obstáculo isolado sob diferentes condições de estabilidade. Thesis Masters. Universidade Federal do Espírito Santo. Vitória, ES, Brazil.

Fluent 15.0 User's guide. Fluent Inc., Canonsburg, PA, USA, 2013.

Hargreaves, D. M.; Wright N.G. 2007. "On the use of the k-ε model in commercial CFD software to model in neutral atmospheric boundary layer". Journal of wind Engeneering, vol.95, pp. 355-369.

Henderson, S. B., 2013. "Differences in heat-related mortality across four ecological regions with diverse urban, rural, and remote populations in British Columbia, Canada". Health & Place, vol.23, pp. 48-53.

Jones, W. P.; Launder, B. E. 1972. "The prediction of laminarization with two-equation model of turbulence". International Journal of Heat and Mass Transfer. vol. 15. pp. 301-314.

Mavroidis, I., Griffiths, R., Jones, C.; Biltoft, C., 1999. "Experimental investigation of the residence of contaminants in the wake of an obstacle under diferent stability conditions". Atmospheric Environment, vol. 33, pp. 939-949.

Mavroidis, I., Andronopoulos, A., Bartzis, J.G., 2012. "Computational simulation of the residence of air pollutants in the wake of a 3-dimensional cubical building. The effect of atmospheric stability". Atmospheric Environment, No. 63, pp. 189-202.

Menter, F., 1994. "Two-equation eddy-viscosity turbulence models for engineering". AIAA-Journal, vol. 32.

Pope, S., 2000. Turbulent flows. New York: Press Syndicate of the University of Cambridge.

Rocha, P.; Rocha, H.; Carneiro, F.; Silva, M. 2014. "k-ω SST (Shear Stress Transport) turbulence model calibration: A case study on small scale horizontal axis wind turbine". Energy. No. 65, pp. 412-418.

Santos, J., 2000. Flow and Dispersion Around Isolated Buildings. Ph. D. Thesis. Department of Chemical Engineering. University of Manchester. England.

Tominaga, Y.; Akabayashi, S.; Kitahara, T.; Arinami, Y., 2015. "Air flow around isolated gable-roof pitches: Wind tunnel experiments and CFD simulations". Atmospheric Environment, No. 84, pp. 204-213.

Valger, S.A.; Fedorova, N.N.; Fedorov, A.V., 2015. "Structure of turbulent separated flow in the neighborhood of a plate-mounted prism of square section". Thermophysics and Aeromechanics, No. 1, vol. 22.

Xing, J.; Zhenyi, L.; Huang, P., 2013. "Experimental and numerical study of the dispersion of carbon dioxide plume. Journal of Hazadous Materials". pp. 256-257.

Yassin, M., 2013. "Wind tunnel study on the effect of thermal stability on flow and dispersion of roof top stack emissions in the near wake of a building". Atmospheric Environment. No. 65, pp. 89-100.

7. RESPONSIBILITY NOTICE

The authors are the only responsible for the printed material included in this paper.